

The Evaluation of Potentiostats: Electrochemical Detection Devices

N. A. Abdul-Kadir¹, S. Noi¹ and F. K. Che Harun^{1,2}

¹Faculty of Biosciences and Medical Engineering, Universiti Teknologi Malaysia,
81310 UTM Johor Bahru, Johor Bahru, Malaysia.

²Faculty of Electrical Engineering, Universiti Teknologi Malaysia, 81310 UTM Johor Bahru, Johor Bahru, Malaysia.
fauzan@utm.my

Abstract—This study evaluated the performance of three types of potentiostats; EmStat, CheapStat and UTMStat. EmStat is the smallest potentiostat available in the market. CheapStat is an open-source potentiostat suitable for educational applications. In addition, UTMStat is the extension of CheapStat, which was designed to overcome few weaknesses of CheapStat such as the input controller/ switch and data storage handling of the cyclic voltammogram. The cyclic voltammetry and amperometry measurements of ions ferrocyanide ($[\text{Fe}(\text{CN})_6]^{4-}$) and chloride (Cl^-) were carried out for each potentiostat. EmStat potentiostat is not only able to detect but also to measure ferrocyanide and chloride ions. However, CheapStat and UTMStat are only able to detect and measure ferrocyanide ions. The experiment is unable to be conducted due to limitation of waveform selection on both devices. Nevertheless, CheapStat and UTMStat could provide a reliable measurement to realize miniaturized lab-on-chip applications as shown in this study.

Index Terms—Amperometry; Chloride and Ferrocyanide Ions; Cyclic Voltammogram; Potentiostat.

I. INTRODUCTION

Potentiometric system has always been related to electrochemical detection method [1]. The combination of electrochemical cell and a potentiostat circuit forms a potentiostatic system [2]. Potentiostat is a feedback control system [3] which adjusts the voltage across the WE - CE pair to maintain the preset potential between the WE and RE of an electrochemical cell [4]. Multitude of research activity has been focused on various potentiostat designs such as standard potentiostat [5-8], virtual potentiostat [9], CMOS potentiostat [10-12] and BiCMOS potentiostat [13].

LabVIEW, a program development environment which uses graphical programming language (language G) to program in block diagram form [14] which is developed by National Instruments (NI) and could be used to develop a virtual potentiostat [9]. LabVIEW has been utilized in monitoring system [15-19], converter life prediction system [14], conversion technique simulator [20], data acquisition system [21, 22] and fully automated electromechanical system [23] due to user friendly and rich of graphical interface.

The electrochemical detection method is utilized into the continuous monitoring system due to its specificity, inexpensive, user friendly and portability [24]. A lot of inventions of continuous monitoring to determine a patient's internal condition of physiological systems, such as nervous system, breathing system and blood circulation have been developed. The system is for continuous monitoring of

chloride [25], glucose [26], hydrogen peroxide [27,28], e coli [15], bovine serum albumin [29], pH [30], potassium [30] and blood pressure [31].

It is crucial to monitor the chemicals and biomarkers to predict patients' critical condition especially during surgical procedures and in intensive care units. Monitoring biomarkers could provide information of any abnormalities which have occur in the metabolic pathways of patient. Hence, further understanding or earlier diagnosis could aid clinician or physician.

Therefore, this study is to compare the existing instruments for electrochemical detection. The purpose is to use the selected electrochemical detection device to be integrated with a biomedical device for designing a continuous monitoring lab-on-chip (LOC) device later. LOC device is an integration of at least one laboratory function on a single integrated circuit, such as a micropump and the reaction zone.

II. ELECTROCHEMICAL THEORY

To introduce electrochemistry, the reversible ferricyanide-ferrocyanide couple is commonly used in educational tool [10]. The ferricyanide/ferrocyanide couple is used as a standard to demonstrate cyclic voltammetry (CV). The ferricyanide/ferrocyanide couple requires no any complications of proceeding or post chemical reactions but able to illustrate nearly a reversible electrode reaction, as evidence by [4, 32-34].

From Figure 1, as the potential is in forward scan and is sufficiently positive to oxidize ferrocyanide ions to ferricyanide ions, the oxidation current is due to the electrode process given by Equation (1). The role of the electrode is an oxidant (electron acceptor) and the oxidation current increases to a peak is observed. The concentration of ferrocyanide ions at the electrode surface depletes and the current then decreases.



As the potential is in reverse scan, the potential is still sufficiently positive to oxidize ferrocyanide ions to ferricyanide ions, therefore oxidation current continues. When the role of the electrode is a strong reductant, ferricyanide ions which has been formed will be reduced to ferrocyanide ions, the reduction current is due to the electrode process given by Equation (2). The reduction current increases to a peak and then decays as ferricyanide ions are consumed.



In clinical diagnosis, monitoring of chloride ions is essential because it is a major mineral nutrient in body fluids and a prominent negatively charged ion of the blood [36], therefore when deficiency of chloride occurs, the blood becomes overly alkaline or known as alkalosis which will result in a life-threatening condition.

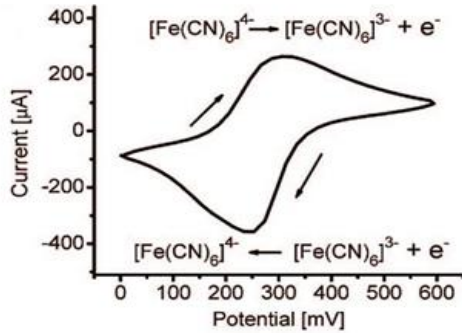


Figure 1: CV for ferricyanide/ferrocyanide couple detection [35]

Figure 2 illustrates CV for chloride ions. As seen in the green line, without the presence of chloride ions, only peak B is observed. Peak B correlates to the one electron oxidation of silver given by Equation (3).



In the presence of chloride ions, two broad peaks (peaks A and B) are observed. The reaction occurs at peak A given by Equation (4). This is proven by observing the peak height of peak A linearly proportional with the concentration of chloride ions. Besides, when the height of peak A increases, the height of peak B decreases. This is due to the reaction at peak A has consumed some of the silver. Therefore, less charge to be passed under peak B.

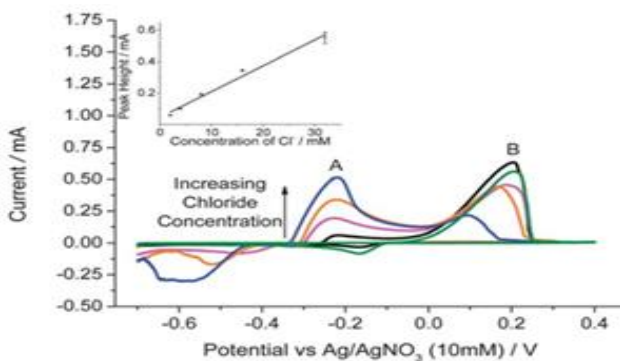
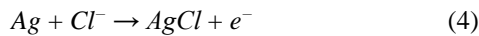


Figure 2: CV for chloride ions detection [37]

Ferrocyanide ions detection does not require any complications of proceeding or post chemical reactions. It can be detected by using any screen printed electrode (SPE). As for chloride ions detection, the SPE used must have silver WE [25, 37].

III. POTENTIOSTAT DEVICES

CV and amperometry techniques have always been related to potentiometric system. In this study, there are three types of potentiostats used: EmStat, CheapStat and UTMStat (modified CheapStat).

A. Potentiostat - EmStat

EmStat (Figure 3) - the smallest potentiostat [38] developed by PalmSens which is controlled and powered by USB and used with the PSTrace software (Figure 4).



Figure 3: EmStat by PalmSens [38]

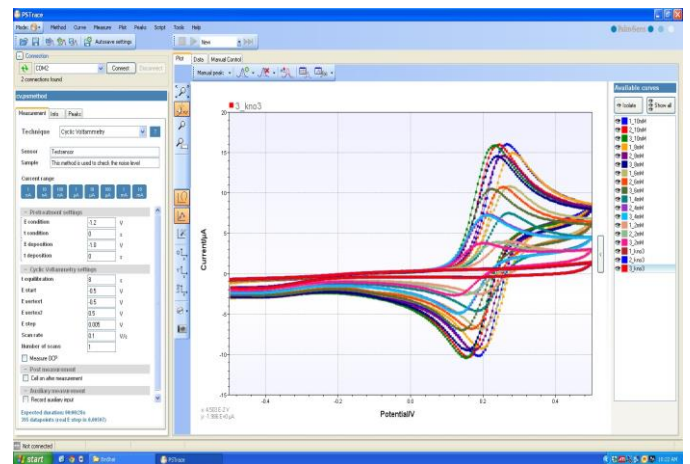


Figure 4: GUI of EmStat

B. Potentiostat - CheapStat

CheapStat (Figure 5) - an open-source potentiostat which is developed by [10]. Same as EmStat, it is controlled and powered by USB. The GUI (Figure 6) is a Java program which receives results from the CheapStat device via USB. CheapStat is a surface-mount device (SMD) which employed surface-mount technology (SMT). The development of CheapStat started by purchasing the electronic components from Element14, formerly Farnell, and Mouser Electronics while the printed circuit board (PCB) was printed by the PCB manufacturer based on the given parts list and schematic diagram in [10]. Then, the electronic components were mounted onto the surface of PCB and the fabricated device as in Figure 5.

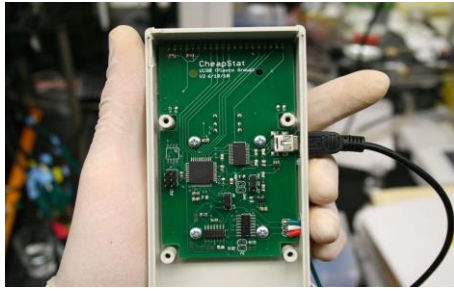


Figure 5: The CheapStat, an inexpensive, “do-it-yourself” potentiostat [10]

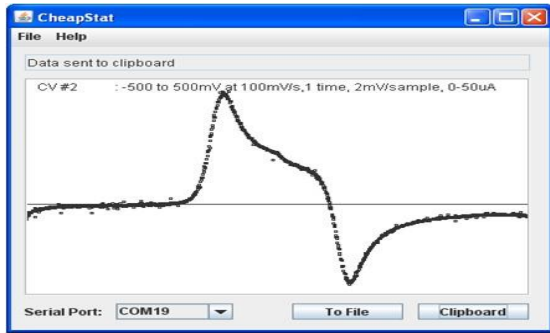


Figure 6: GUI of CheapStat

C. Potentiostat - UTMStat

UTMStat - a LabVIEW based modified CheapStat was developed due to few weaknesses of CheapStat such as the waveform parameters have to be input by controlling the 4-way switch and the cyclic voltammogram and the data points for cyclic voltammogram have to be manually saved onto the computer. Firstly, the input to CheapStat and the output from CheapStat were studied.

In CheapStat source code (CheapStat_v2.c), the waveform parameters are stored in a structure named profile. For example, if selected waveform is CV with 5000 mV/s, potential range from -100 mV to 100 mV, one time scan, 1 mV/sample and 0 – 10 μ A current range are input by controlling the 4-way switch.

In order to observe the output from CheapStat, it was connected to PC via USB. LabVIEW example program (Basic Serial Write and Read.vi) was used to read the output from CheapStat. For example, if selected waveform is CV with 5000 mV/s, potential range from -100 mV to 100 mV, one time scan, 1 mV/sample and 0 - 10 μ A current range are input by controlling the 4-way switch; the output string is shown in Table 1 and Table 2. The output is in word size data (16-bit), therefore MSB and LSB stand for most significant bit and least significant bit respectively.

In Table 1, part of the output is just the waveform parameters. The most important part is listed in Table 2. The output string "\01\EF" shows that there are 495 data points which are needed in drawing the cyclic voltammogram. Integration with LabVIEW started by reading the waveform parameters from the user through Figure 7.

Table 1
Output from CheapStat (Waveform Parameters)

Source code	Output string
USART_PutChar(&USARTC0, CV);	\01
USART_PutChar(&USARTC0, name[j]);	CV\s#1\s\s\s\s\s
	\s\s\s\s\s
USART_PutChar(&USARTC0, slope>>8);	\13
USART_PutChar(&USARTC0, slope);	\88
USART_PutChar(&USARTC0, start>>8);	\FF
USART_PutChar(&USARTC0, start);	\9C
USART_PutChar(&USARTC0, stop>>8);	\00
USART_PutChar(&USARTC0, stop);	d
USART_PutChar(&USARTC0, scans>>8);	\00
USART_PutChar(&USARTC0, scans);	\01
USART_PutChar(&USARTC0, sample_rate>>8);	\00
USART_PutChar(&USARTC0, sample_rate);	\01
USART_PutChar(&USARTC0, curr_range);	\01

Table 2
Output from CheapStat (Data Points)

Source code	Output string
USART_PutChar(&USARTC0, i>>8);	\01
USART_PutChar(&USARTC0, i);	\EF
USART_PutChar(&USARTC0, current[j]>>8);	495 data points
USART_PutChar(&USARTC0, current[j]);	
USART_PutChar(&USARTC0, CV);	\01

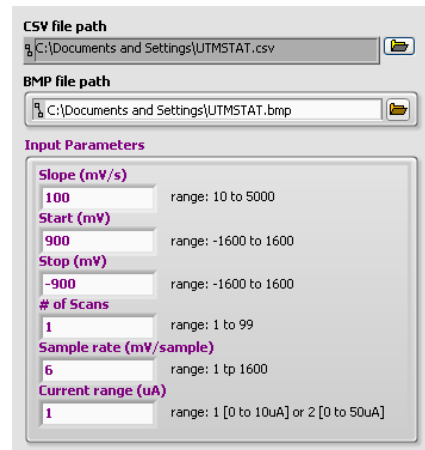


Figure 7: Input from user

In UTMStat, the ISR function in CheapStat_v2.c was modified to read the waveform parameters from LabVIEW. Once all the data had been read, the data was processed in the main function in CheapStat_v2.c. After all waveform parameters were stored, CV_test function was invoked. UTMStat sent the output to LabVIEW program. Firstly, 27 bytes of data (Table 1) was discarded. The next data obtained was the data point size and followed by current data points which needed in drawing the cyclic voltammogram. Since the data was in word size data, the total current data points which needed to be read was multiplication of data point size by 2. Both files were saved automatically on the computer at the selected paths (Figure 7).

Therefore, by enhancing CheapStat, the waveform parameters can be input easily through the LabVIEW. The cyclic voltammogram and the data point can be saved into BMP (Figure 8) and CSV files automatically. Comparisons among the three potentiostats: EmStat, CheapStat and UTMStat are shown in Table 3.

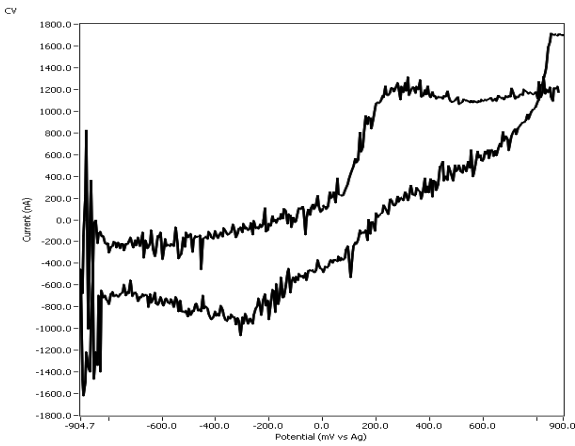


Figure 8: BMP file

Table 3
Comparisons of Potentiostats

Specifications	EmStat	CheapStat	UTMStat
Number of potential waveforms	15	6	6
Current range	1 nA to 10 mA	~100 nA to ~50 µA	~100 nA to ~50 µA
Potential range	± 3.000 V	± 1.600 V	± 1.600 V
Price	~RM 8800	~RM 230	~RM 230

IV. EVALUATION OF POTENTIOSTAT

The CV and amperometry measurements of ions ferrocyanide ($[Fe(CN)_6]^{4-}$) and chloride (Cl^-) were carried out. The results from the EmStat, CheapStat and UTMStat are as follow.

1. EmStat - Ferrocyanide & Chloride Ions Detections

A. Ferrocyanide Ions Detection

The CV measurement of various concentrations range 2-10 mM, in 2 mM increments of potassium ferrocyanide in 1 M potassium nitrate at a scan rate of 0.1 V/s had been carried out using EmStat and the result is shown in Figure 9. According to Levich theory, the peak current is directly proportional to the concentration of the species; therefore 10 mM potassium ferrocyanide achieved the highest oxidation peak of 15.22945 µA at potential 0.25 V, as shown in Figure 9 and Table 4.

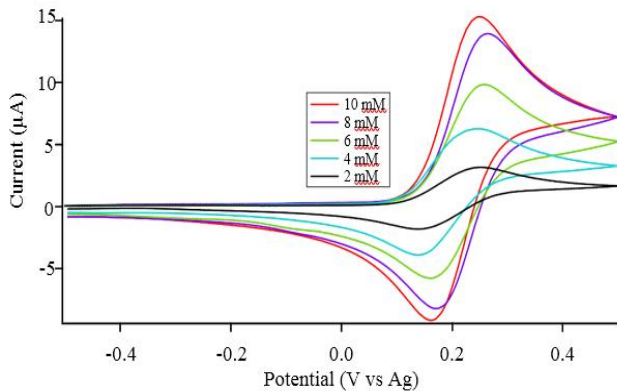


Figure 9: Background-subtracted cyclic voltammometry-based monitoring of potassium ferrocyanide in 1 M potassium nitrate using EmStat [24]

Table 4

Oxidation peak current at potential 0.25 V of various concentration of potassium ferrocyanide in 1 M potassium nitrate using EmStat [24]

Concentration (mM)	Current (µA)
10	15.22945
8	13.61254
6	9.72236
4	6.20588
2	3.10379

For amperometry measurement of various concentrations range 2-10 mM, in 2 mM increments of potassium ferrocyanide in 1 M potassium nitrate had been carried out using EmStat and the result is shown in Figure 10. The constant applied voltage of 0.25 V was chosen based on the result in Figure 9 and the duration is 60 seconds. According to Levich theory, the current is directly proportional to the concentration of the species; therefore 10 mM potassium ferrocyanide obtained the highest average current at 3.46672 µA, as shown in Figure 10 and Table 5.

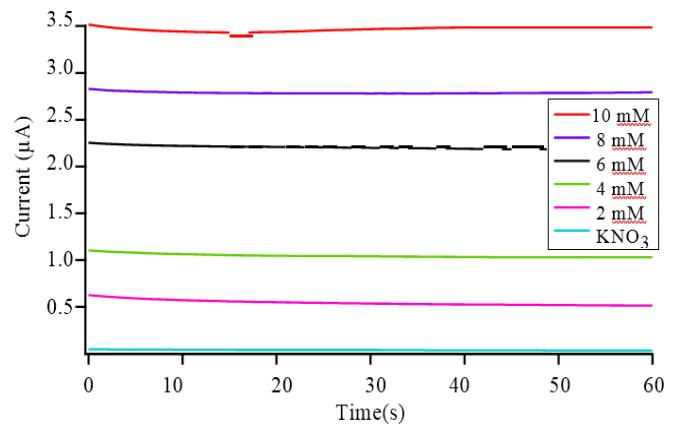


Figure 10: Amperometry-based monitoring of potassium ferrocyanide in 1 M potassium nitrate using EmStat.

Table 5

Average oxidation peak current at potential 0.25 V using EmStat

Concentration (mM)	Average Current (µA)
10	3.46672
8	2.78650
6	2.20068
4	1.04415
2	0.54273
0	0.03699

The CV measurement was extended by various concentrations range 2-10 mM, in 2 mM increments of potassium ferrocyanide in 0.1 M potassium nitrate at a scan rate of 0.1 V/s had been carried out using EmStat and the result is shown in Figure 11. According to Levich theory, the peak current is directly proportional to the concentration of the species; therefore 10 mM potassium ferrocyanide achieved the highest oxidation peak of 10.18181 µA at potential 0.32 V, as shown in Figure 11 and Table 6.

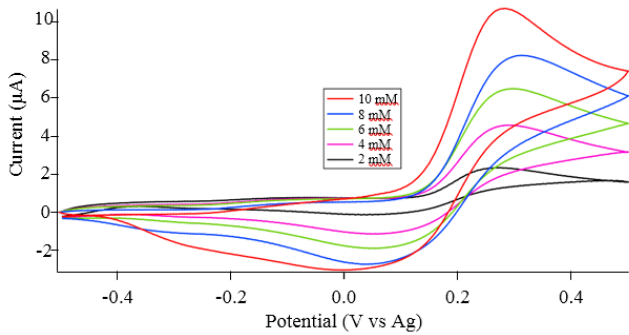


Figure 11: Background-subtracted cyclic voltammetry-based monitoring of potassium ferrocyanide in 0.1 M potassium nitrate using EmStat

Table 6

Oxidation peak current at potential 0.32 V of various concentration of potassium ferrocyanide in 0.1 M potassium nitrate using EmStat

Concentration (mM)	Current (µA)
10	10.18181
8	8.21473
6	6.39368
4	4.46598
2	2.20702

The amperometry measurement was furthered by various concentrations range 2-10 mM, in 2 mM increments of potassium ferrocyanide in 0.1 M potassium nitrate had been carried out using EmStat and the result is shown in Figure 12. The constant applied voltage of 0.32 V was chosen based on the result in Figure 11 and the duration is 60 seconds. According to Levich theory, the current is directly proportional to the concentration of the species; therefore 10 mM potassium ferrocyanide obtained the highest average current at 2.98336 µA, as shown in Figure 12 and Table 7.

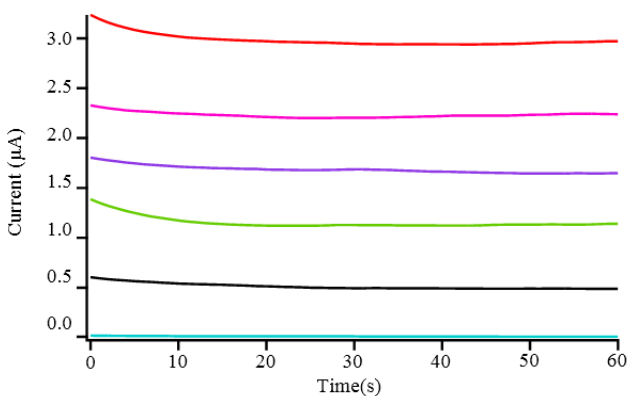


Figure 12: Amperometry-based monitoring of potassium ferrocyanide in 0.1 M potassium nitrate using EmStat

Table 7

Average oxidation peak current at potential 0.32 V using EmStat

Concentration (mM)	Current (µA)
10	2.98336
8	2.23123
6	1.68447
4	1.15318
2	0.51247
0	0.01128

B. Chloride Ions Detection

The CV measurement of various concentrations range 10-50 mM, in 10 mM increments of potassium chloride in 0.1 M potassium nitrate at a scan rate of 0.05 V/s had been carried out using EmStat and the result is shown in Figure 13. To have a clear view of Figure 13, another cyclic voltammogram of Figure 13 was recorded from +0.00 V to +0.20 V (Figure 14). According to Levich theory, the peak current is directly proportional to the concentration of the species; therefore 50 mM potassium chloride achieved the highest oxidation peak of 114.10837 µA at potential 0.13 V, as shown in Figure 13, Figure 14 and Table 8.

The formal potential of the redox couple of Ag/AgCl (4) was +0.32 V vs. NHE and the redox potential of chloride ions was measured at -0.25 V [37]. In this study experiment, the redox potential of chloride ions was achieved at +0.13 V. The difference is due to the type of reference electrode used. [37] used Ag/Ag (10 mM) and NaNO₃ (90 mM) reference electrode while Ag/AgCl was used as the reference electrode in this experiment. The potential of the redox pair of Ag/Ag⁺ (3) was +0.69 V vs. NHE but the potential of the redox pair of Ag/AgCl was +0.197 V vs. NHE.

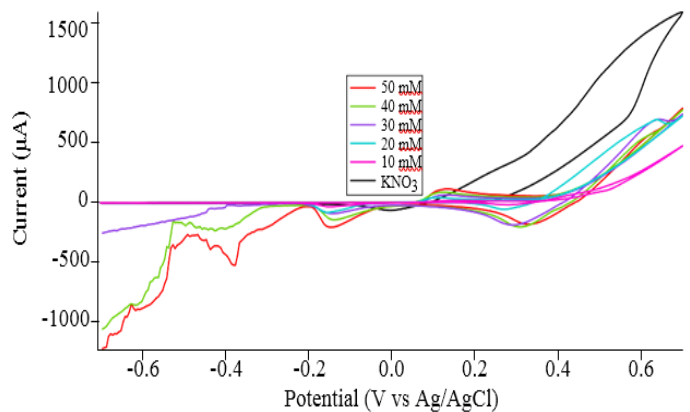


Figure 13: Cyclic voltammetry-based monitoring of potassium chloride in 0.1 M potassium nitrate using EmStat

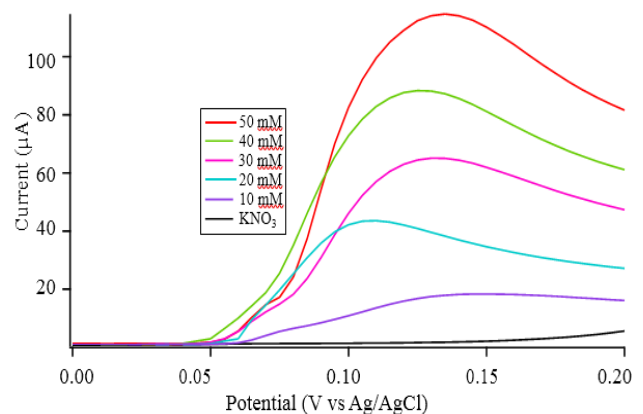


Figure 14: Cyclic voltammetry-based monitoring of potassium chloride in 0.1 M potassium nitrate using EmStat from +0.00 V to +0.20 V

Table 8

Oxidation peak current at potential 0.13 V of various concentration of potassium chloride in 0.1 M potassium nitrate using EmStat

Concentration (mM)	Current (µA)
10	114.10837
8	88.16505
6	65.05255
4	39.54370
2	17.45438
0	1.67044

Theoretically, the electrode potentials were converted to the NHE scale using Equation (5) [39]. By using (5) and the formal potential of the redox couple of Ag/AgCl (4) was +0.32 V vs. NHE [37], the formal redox potential of chloride ions should have a theoretical potential at +0.123 V; which was close to the experimentally measured at +0.13 V.

$$E(NHE) = E(Ag/AgCl) + 0.197 V \quad (5)$$

2. CheapStat - Ferrocyanide Ions Detection

The CV measurement of various concentrations range 2-10 mM, in 2 mM increments of potassium ferrocyanide at a scan rate of 0.1 V/s was tested using Cheapstat and the result is illustrated in Figure 15. According to Levich theory, the peak current is directly proportional to the concentration of the species; therefore the highest peak current at potential 0.25 V was achieved by 10 mM potassium ferrocyanide at 0.41033 µA as shown in Figure 15 and Table 9.

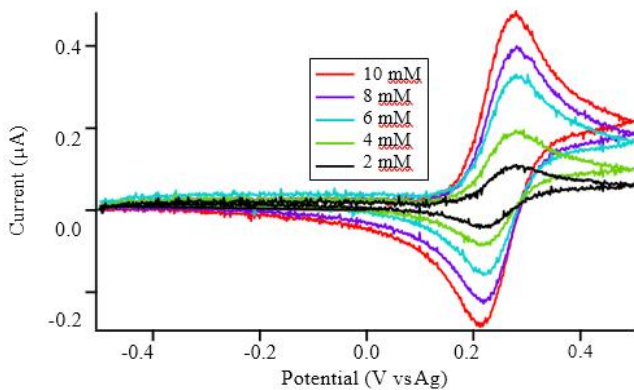


Figure 15: Amperometry-based monitoring of potassium ferrocyanide in 0.1 M potassium nitrate using EmStat

Table 9

Oxidation peak current at potential 0.25 V using CheapStat

Concentration (mM)	Current (µA)
10	0.41033
8	0.32733
6	0.27500
4	0.16467
2	0.09033

The amperometry measurement of various concentrations range 2-10 mM, in 2 mM increments of potassium ferrocyanide in 1 M potassium nitrate using CheapStat was not carried out due the waveform selection was not available in CheapStat.

3. UTMStat - Ferrocyanide Ions Detection

The CV measurement of various concentrations range 2-10 mM, in 2 mM increments of potassium ferrocyanide at a scan rate of 0.1 V/s was tested using UTMStat and the result is illustrated in Figure 16. According to Levich theory, the peak current is directly proportional to the concentration of the species; therefore the highest peak current at potential 0.25 V was obtained by 10 mM potassium ferrocyanide at 0.43233 µA as shown in Figure 16 and Table 10.

In this study, the amperometry measurement of various concentrations range 2-10 mM, in 2 mM increments of potassium ferrocyanide in 1 M potassium nitrate using UTMStat was not performed because the waveform selection is not available in original CheapStat.

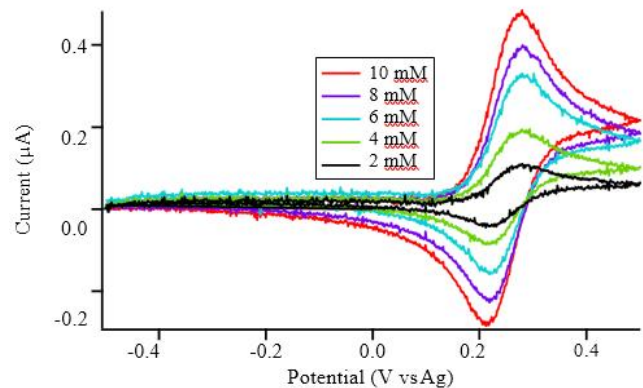


Figure 16: Background-subtracted cyclic voltammetry-based monitoring of potassium ferrocyanide in 1 M potassium nitrate using UTMStat

Table 10

Oxidation peak current at potential 0.25 V using UTMStat

Concentration (mM)	Current (µA)
10	0.43233
8	0.33133
6	0.22767
4	0.19467
2	0.09167

V. DISCUSSIONS

The electrochemical detection of ferrocyanide ions is compared among three potentiostats: EmStat from PalmSens, CheapStat [10] and in house UTMStat.

UTMStat is actually an extension of existing CheapStat integrated with LabVIEW program to overcome few drawbacks of CheapStat such as the waveform parameters have to be input by controlling the 4-way switch and the cyclic voltammogram and the potential-current pair data points have to be manually saved onto the computer. Therefore, by enhancing CheapStat, the waveform parameters can be input easily through the LabVIEW. Additionally, the CV and the potential-current pair data points can be saved into BMP CSV files automatically at the desired folder path.

The CV measurement of various concentrations range 2-10 mM, in 2 mM increments of potassium ferrocyanide in 1 M potassium nitrate at a scan rate of 0.1 V/s has been carried out using EmStat. 10 mM potassium ferrocyanide achieves the highest oxidation peak of 15.22945 µA at

potential 0.25 V.

The constant applied voltage of 0.25 V is then used in amperometry measurement of various concentrations range 2-10 mM, in 2 mM increments of potassium ferrocyanide in 1 M potassium nitrate. The highest average current at 3.46672 μA is obtained by 10 mM potassium ferrocyanide.

The CV measurement is extended by various concentrations range 2-10 mM, in 2 mM increments of potassium ferrocyanide in 0.1 M potassium nitrate at a scan rate of 0.1 V/s. 10 mM potassium ferrocyanide achieves the highest oxidation peak of 10.18181 μA at potential 0.32 V.

The constant applied voltage of 0.32 V is then used in amperometry measurement of by various concentrations range 2-10 mM, in 2 mM increments of potassium ferrocyanide in 0.1 M potassium nitrate. 10 mM potassium ferrocyanide exhibits the highest average current of 2.98336 μA .

As for chloride ions detection, the CV measurement of various concentrations range 10-50 mM, in 10 mM increments of potassium chloride in 0.1 M potassium nitrate at a scan rate of 0.05 V/s has been carried out. 50 mM potassium chloride shows the highest oxidation peak of 114.10837 μA at potential of 0.13 V; which is close to theoretical potential at 0.123 V.

The CV measurement of various concentrations range 2-10 mM, in 2 mM increments of potassium ferrocyanide at a scan rate of 0.1 V/s is also tested using CheapStat and UTMStat where 10 mM potassium ferrocyanide achieves the highest oxidation peak of 0.41033 μA and 0.43233 μA at potential 0.25 V respectively.

The amperometry measurement for both CheapStat and UTMStat is not performed because waveform selection is not available in the original CheapStat.

VI. CONCLUSION

The evaluation of three potentiostats has been done using EmStat, CheapStat and UTMStat in this study. CheapStat and UTMStat are LabVIEW based potentiostat, whereas UTMStat is the improved version of open-source CheapStat potentiostat. EmStat is expensive compared to CheapStat and UTMStat. The oxidation peak current at potential 0.25 V using CheapStat and UTMStat are almost similar (2 to 10 mM concentration able to measure current at 0.09 to 0.4 μA). Nevertheless, UTMStat could provide a reliable measurement to further realize miniaturized lab-on-chip applications.

ACKNOWLEDGMENT

The authors would like to thank the Ministry of Higher Education Malaysia and Universiti Teknologi Malaysia for supporting and funding this study under Research University Grant No. Q.J130000.2601.14J50.

REFERENCES

- [1] G. S. Wilson and M. A. Johnson, "In-vivo electrochemistry: What can we learn about living systems?," *Chem. Rev.*, vol. 108, pp. 2462–2481, Jul 2008.
- [2] J. C. Fidler, W. R. Penrose, and J. P. Bobis, "A potentiostat based on a voltage-controlled current source for use with amperometric gas sensors," *IEEE Trans. Instrum. Meas.*, vol. 41, no. 2, pp. 308–310, Apr 1992.
- [3] P. M. Levine, P. Gong, R. Levicky, and K. L. Shepard, "Active CMOS sensor array for electrochemical biomolecular detection," *IEEE J. Solid-State Circuits*, vol. 43, no. 8, pp. 1859–1871, Aug 2008.
- [4] A. Bard; L. Faulkner, *Electrochemical methods: fundamentals and applications*. John Wiley & Sons: New York, 1980.
- [5] M. Paeschke, F. Dietrich, A. Uhlig, and R. Hintsche, "Voltammetric multichannel measurements using silicon fabricated microelectrode arrays," *Electroanalysis*, vol. 8, no. 10, pp. 891–898, Oct 1996.
- [6] Ramfos, N. Vassiliadis, S. Bionas, K. Efstathiou, A. Fragoso, C. K. O'Sullivan, and A. Birbas, "A compact hybrid-multiplexed potentiostat for real-time electrochemical biosensing applications," *Biosens Bioelectron*, vol. 47, pp. 482–489, Sep 2013.
- [7] M. Vergani, M. Carminati, G. Ferrari, E. Landini, C. Caviglia, A. Heiskanen, C. Comminges, K. Zor, D. Sabourin, M. Dufva, M. Dimaki, R. Raiteri, U. Wollenberger, J. Emnéus, and M. Sampietro, "Multichannel bipotentiostat integrated with a microfluidic platform for electrochemical real-time monitoring of cell cultures," *IEEE Trans. Biomed. Circuits Syst.*, vol. 6, no. 5, pp. 498–507, Oct 2012.
- [8] M. A. Tapsak, J. G. Houseknecht, and P. V. Goode, "A low cost computer controlled and powered multichannel potentiostat for general use in development of inexpensive electrochemical sensors," *J. Instrumentation Science & Technology*, vol. 35, issue 6, pp/ 589-598, Oct 2007.
- [9] F. J. Sun and J. Wang, "Development and application of virtual potentiostat on electrochemical corrosion measurement," *Acta Physico-Chim. Sin.*, vol. 28, no. 3, pp. 615–622, Mar 2012.
- [10] A. A. Rowe, A. J. Bonham, R. J. White, M. P. Zimmer, R. J. Yadgar, T. M. Hobza, J. W. Honea, I. Ben-Yaacov, and K. W. Plaxco, "CheapStat: An open-source, "Do-it-yourself" Potentiostat for analytical and educational applications," *PLoS one*, vol. 6, p. e23783, Jan 2011.
- [11] S. Hwang and S. Sonkusale, "CMOS VLSI potentiostat for portable environmental sensing applications," *IEEE Sensors J.*, vol. 10, no. 4, pp. 820–821, Apr 2010.
- [12] A. Gore, S. Chakrabarty, S. Pal, and E. C. Alocilja, "A multichannel femtoampere-sensitivity potentiostat array for biosensing applications," *IEEE Trans. Circuits Syst I: Regular Papers*, vol. 53, no. 11, pp. 2357–2363, Nov 2006.
- [13] R. Genov, M. Stanacevic, M. Naware, G. Cauwenberghs, and N. V. Thakor, "16-Channel integrated potentiostat for distributed neurochemical sensing," *IEEE Trans. Circuits Syst. I: Regular Papers*, vol. 53, no. 11, pp. 2371–2376, Nov 2006.
- [14] Z. Shihong, G. Yong, W. Lifeng, P. Wei, W. Guohui, and D. Yinyu, "Design and realization of dc-dc converter life prediction system based on labview," *J. Convergence Information Technology*, vol. 6, no. 11, pp. 300, Nov 2011.
- [15] X. Muñoz Berbel, R. Escudé-Pujol, N. Vigués, M. Cortina-Puig, C. García-Aljaro, J. Mas, and F. X. Muñoz, "Real time automatic system for the impedimetric monitoring of bacterial growth," *J. Analytical Letters*, vol. 44, no. 16, pp. 2571-2581, Nov. 2011.
- [16] Han and S. Song, "A measurement system based on electrochemical frequency modulation technique for monitoring the early corrosion of mild steel in seawater," *Corrosion Science*, vol. 50, no. 6, pp. 1551–1557, Jun 2008.
- [17] Yi, Z. Feng, L. Gang, and W. Kai, "The real-time monitor system based on LabVIEW," *Int. Conf. Computer Science and Network Technology (ICCSNT)*, China, 2011, vol. 2, pp. 848–851.
- [18] A. Chouder, S. Silvestre, B. Taghezouit, and E. Karatepe, "Monitoring, modelling and simulation of PV systems using LabVIEW," *Solar Energy*, vol. 91, pp. 337–349, May 2013.
- [19] N. Sahgal, "Monitoring and analysis of lung sounds remotely," *Int. J. Chron. Obstruct. Pulmon. Dis.*, vol. 6, no. 1, pp. 407–412, Jul 2011.
- [20] A. Odon and Z. Krawiecki, "LabVIEW application for computer simulation of the conversion technique of dual-slope analog-to-digital converter," *Measurement*, vol. 44, no. 8, pp. 1406–1411, Oct 2011.
- [21] A. Bozatzidis, A. G. Anastopoulos, and T. Laopoulos, "Automated data acquisition setup for interfacial tension and capacitance measurements at Hg- solution contacts under LabVIEW control," *Electroanalysis*, vol. 19, no. 16, pp. 1711–1718, Jul 2007.
- [22] W. Lijun, X. Long, and Z. Jianbin, "Multi-channel peripheral data acquisition system based on LabVIEW and SCM," *J. Convergence Information Technology*, vol. 7, no. 22, Dec 2012.
- [23] I. A. Rojas-Olmedo, R. López-Callejas, A. de la Piedad-Beneitez, R. Valencia-Alvarado, R. Peña Eguiluz, A. Mercado-Cabrera, S. R. Barocio, A. E. Muñoz Castro, and B. G. Rodríguez-Méndez, "An automated system for DC and RF plasma characterization by guard double electric probes," *Surface and Coatings Technology*, vol. 205, no. 2, pp. S397–S401, Jul 2011.
- [24] S. Noi, P. S. Chee, F. K. Che Harun, P. L. Leow, and A. Aziz, "Integration of electrochemical detection into micropumps for

- continuous monitoring system,” *Proc. 10th Asian Control Conf. 2015 (ASCC 2015)*, Malaysia, 2015, pp. 1658–1662.
- [25] L. Trnkova, V. Adam, J. Hubalek, P. Babula, and R. Kizek, “Amperometric sensor for detection of chloride ions,” *Sensors*, vol. 8, pp. 5619–5636, Sept. 2008.
- [26] R. Dutt-Ballerstadt, C. Evans, A. P. Pillai, and A. Gowda, “A label-free fiber-optic Turbidity Affinity Sensor (TAS) for continuous glucose monitoring,” *Biosens. Bioelectron.*, vol. 61, pp. 280–284, Nov. 2014
- [27] I. Rodríguez-Ruiz, E. Masvidal-Codina, T. N. Ackermann, and A. Llobera, “Photonic lab-on-chip (PhLOC) for enzyme-catalyzed reactions in continuous flow,” *Microfluid Nanofluidics*, vol. 18, no. 5-6, pp. 1277–1286, May 2015.
- [28] R. Ferrigno and P. Pittet, “Combining microfluidics and electrochemical detection,” *Annual Int. Conf. IEEE Eng. Med. Biol. Soc. EMBC2009*, Minneapolis, USA, 2009, pp. 4144–4146.
- [29] A. Nilghaz, D. H. B. Wicaksono, D. Gustiono, F. A. Abdul Majid, E. Supriyanto, and M. R. Abdul Kadir, “Flexible microfluidic cloth-based analytical devices using a low-cost wax patterning technique,” *Lab Chip*, vol. 1, Jan 2012.
- [30] B. Tahirbegi, M. Mir, S. Schostek, M. Schurr, and J. Samitier, “In vivo ischemia monitoring array for endoscopic surgery,” *Biosens. Bioelectron.*, vol. 61, pp. 124–130, Nov. 2014.
- [31] Hassan and M. Mashor, “A portable continuous blood pressure monitoring kit,” *IEEE Symp. Business. Eng. Industrial Applications (ISBEIA) 2011*, Malaysia, 2011, pp. 503–507.
- [32] R. S. Nicholson and I. Shain, “Theory of stationary electrode polarography. Single scan and cyclic methods applied to reversible, irreversible, and kinetic systems,” *Anal. Chem.*, vol. 36, no. 4, pp. 706–723, Apr 1964.
- [33] S. W. Feldberg, “Digital simulation: a general method for solving electrochemical diffusion-kinetic problems,” *Electroanalytical Chem.*, vol. 3, pp. 199–296, 1969.
- [34] D. K. Gosser, “Cyclic voltammetry: simulation and analysis of reaction mechanisms,” *J. Synth. React. Inorg. Met-Org. Chem.*, vol. 24, no. 7, pp. 1235–1236, 1994.
- [35] D. Grieshaber, J. Vörös, T. Zambelli, V. Ball, P. Schaaf, J.-C. Voegel, and F. Boulmedais, “Swelling and contraction of ferrocyanide-containing polyelectrolyte multilayers upon application of an electric potential,” *Langmuir*, vol. 24, no. 23, pp. 13668–13676, Oct 2008.
- [36] T. Kokubo and H. Takadama, “How useful is SBF in predicting in vivo bone bioactivity?” *Biomaterials*, vol. 27, no. 15, pp. 2907–15, May 2006.
- [37] H. S. Toh, C. Batchelor-mcauley, K. Tschulik, and R. G. Compton, “Electrochemical detection of chloride levels in sweat using silver nanoparticles: A basis for the preliminary screening for cystic fibrosis,” *The Analyst*, vol. 138, no. 15, pp. 4292–7, 2013.
- [38] PalmSens.com ‘PalmSens Compact Electrochemical Interfaces’, [online]. Available: <https://www.palmsens.com/product/emstat/>. [Accessed: 21 July 2014]
- [39] J. Esswein, Y. Surendranath, S. Y. Reece, and D. G. Nocera, “Highly active cobalt phosphate and borate based oxygen evolving catalysts operating in neutral and natural waters,” *Energy Environ. Sci.*, issue 2, pp. 499–504, Feb 2011.